Fluid and aero-acoustic analysis of internal bays: geometric length-to-depth effects

Zumra Zainab and *Adnan Maqsood* *

National University of Sciences and Technology, Islamabad, Pakistan

Abstract. Weapon bays are essential for any bomber, Next Generation Fighter Aircraft, and unmanned combat air vehicles (UCAVs). As flow approaches the leading edge of such cavity, it separates and forms a shear layer. The structure of bays and residing stores thus become prone to intense acoustic and aerodynamic loading– a major design concern. Cavity flow shows significant dependence on its shape. This makes flow actuation possible by only changing the geometric variable of length-to-depth (L/D) ratio. This study compares two bays with an L/D ratio of 5 (deep) and 10 (shallow) in terms of acoustics and affiliated aerodynamic drag. A transient RANS formulation obtained overall sound pressure levels (OASPL) on bay ceilings. An integral-based method was also used to predict far-field noise propagation due to flow fields of both cavities. It is argued that at Mach 0.6, the character of bays changes remarkably when its L/D is altered. Deeper bays show a smoother pressure profile and significantly less drag while operating in shear mode. Shallow bays, on the other hand, show bluff body type drag with uneven pressure distribution, having the potential of causing downwash on residing stores. At the same time, acoustic loads on the ceiling and acoustic signatures in the far-field are comparable for both cavities.

1 Introduction

Most aircraft carry stores in external configurations. However, this external weapon carriage configuration can increase the aircraft's drag by up to 30% and make it more easily detectable by radar [1]. The future generations of aircraft must have internal storage capability, low acoustic and radar signature, and post-stall maneuverability. However, the design and presence of weapon bays and stores can lead to complex cavity-driven fluid and aero-acoustic characteristics that must be analyzed for safety. This requires extensive study into various configurations of bays to perform well in most flight envelopes. Cavity flows are not only an aircraft design problem but are found in various other applications. Besides weapons bays, landing gear compartments, and cavity-like structures such as aircraft window panels, antenna housing also follows cavity flow dynamics. The phenomenon of acoustic resonance in Safety relief valves is often encountered in industries. Acoustics resonance of engine cavities is also a significant concern. As the boundary layer reaches the leading wall of a

* Corresponding author: adnan@sines.nust.edu.pk

cavity, it separates and forms a shear layer between flow within bays and freestream flow. This shear layer sheds vortices and causes static pressure variations. Studying the behavior of the shear layer can help categorize such flows. Many studies in the literature have found that whether the shear layer will bridge the bay or sag into it depends on the length-to-depth ratio [2]. A bay with lower L/D tends to form a significant recirculation region with a shear layer stagnating on the trailing wall.

On the other hand, with increased L/D, the shear layer attaches to the cavity ceiling and then separates before reaching the trailing wall. Naturally, flows within such geometries fluctuate, capable of random and periodic fluctuations at various frequencies [3]. Because of such distribution, fatal resonance can occur if the frequency of flow and natural frequency of structure align. Low-magnitude vibrations are also capable of causing fatigue damage, reducing the life span and integrity of the structure [4]. All in all, the seemingly simple geometry of a 3d cavity causes design concerns and safety issues. Even at Mach, as low as 0.2, relatively deeper bays have shown an intense acoustic environment [5]. Instability within flow drives various phenomena that not only generate an acoustics impact on the surface of the cavity but also propagate noise in mid to far fields.

M219 deep cavity case at Mach 0.95 has become a standard for cavity flow studies [6]. Many authors have investigated OASPL loads on its ceiling. However, to the best of the authors' knowledge, fewer studies are computationally investigating M219 deep cavity flows at 0.6 Mach. There are no studies on M219 shallow bay. This research aims to provide a detailed comparative analysis of these two bay configurations.

2 Theoretical Background

When low-speed flow passes over cavities, they might operate in either wake mood or shear layer mode [7]. In the wake mood, the cavity's shear layer stagnates at some point on the cavity's ceiling before trailing the wall. Such bays will show a drastic increase in drag as self-oscillations stop and flow becomes unstable on a large scale. In shear layer mode, periodic self-sustained oscillations are observed as the feedback loop develops. The shear layer spanning cavity is prone to Kelvin-Helmholtz instabilities, identified as the shear layer rolling onto itself and generating vortices. In addition to KH instabilities, flow experiences centrifugal instability within recirculating regions [5]. These instabilities further amplify streamwise while the acoustic field travels upstream. Research investigating the effect of Mach number on cavity flows concluded that an increase in Mach number in the subsonic regime destabilizes the shear layer [8]. Similarly, as Reynold's number increases, the shear layer destabilizes earlier, increasing fluctuations and fluctuating pressure loads. Disturbance in static pressure fields leads to longitudinal pressure gradients that are known to cause pitching moments on residing stores and weapons [9]. Realistically, problems affiliated with bay flows can be solved by studying the design and geometric shape of the cavity [10]. The effect of the L/D ratio on these flows and at what L/D a cut-off between deep and shallow bays happens has been a topic of interest since the 1960s [3]. This, however, does not make the study easier as other parameters, such as flow regime, come into play. Rossiter [3] was the first to propose a detailed explanation of the contributions of flow and geometric variables. He concluded that periodic fluctuations dominate relatively deep bays, whereas random features are apparent in shallower bays.

Besides vibrations and resonance-induced loading on structures, cavity flows also propagate noise in mid to far field. Aerodynamic noise generation and its propagation have been studied in the literature. Computationally intensive methods like Direct Numerical Simulation (DNS) and Large Eddy Simulation (LES) have shown satisfactory results in predicting noise. However, due to cost and limited studies, these researches mainly cover 2D cavities. Another approach uses an integral-based method utilizing Lighthills's acoustic

analogy by empirically predicting sound propagation from a transient RANS simulation. Gloerfelt et al. [11] compared the DNS solution of 2d cases with integral-based methods, including Ffowcs-Williams and Hawkings (FW-H) model. It was concluded that these approaches give good enough estimation while saving cost. Aerodynamic sound generation is different from sound produced due to the vibration of rigid bodies. Lighthill [12] first asserted that most sound generation studies focused on the fact that acoustic power is the function of operating parameters, and its relation to the flow field must also be investigated. This analogy determines sound radiating from a fluctuating flow field. It is established by separating flow solution and acoustic analysis, meaning sound propagation and sound generation are treated separately. Considering a listener (receiver) in far-field such that flow is uniform and stagnant in the surroundings, an acoustic field can be defined as:

$$\frac{\partial^2 \acute{\rho}}{\partial^2 t} - a_0^2 \nabla^2 \acute{\rho} = 0 \qquad (1)$$

where fluctuating density is derived from;

$$\rho = \rho_{mean} + \acute{\rho} \qquad (2)$$

$$\frac{\partial^2 \acute{\rho}}{\partial^2 t} - \frac{\partial^2 \rho u_i u_j}{\partial x_i \partial x_j} = \frac{\partial^2 p}{\partial x_i^2} - \frac{\partial^2 \tau_{ij}}{\partial x_i \partial x_j} \qquad (3)$$

Equation (3) shows the relationship between the wave equation and acoustic sources. However, it can only be defined as noise produced by free turbulence with no solid boundary.

$$\frac{\partial^2 \rho}{\partial t^2} - a_0^2 \frac{\partial^2 \rho}{\partial x_i^2} = \frac{\partial^2 T_{ij}}{\partial x_i \partial x_j} \qquad (4)$$

T_{ij} is stress tensor given as;

$$T_{ij} = \rho u_i u_j - \tau_{ij} + (p - a_0^2 \rho)\delta_{ij} \qquad (5)$$

FW-H is an integral-based method that provides extension by considering no-slip walls and moving references. It can be used as an alternative to direct simulation for determining noise at mid to far-field by equivalent sources of monopoles, dipoles, and quadrupoles. FW-H is an inhomogeneous wave equation that Navier Stokes and continuity equations can derive. It requires unsteady computation of flow variables such as density, velocity, and pressures on sound sources to obtain surface integral and allow formulation for multiple sources and moving receivers. FW-H equation is given as:

$$\frac{1}{a_0^2}\frac{\partial^2 \acute{p}}{\partial t^2} - \nabla^2 \acute{p} = \frac{\partial^2}{\partial x_i \partial x_j}\{T_{ij} H(f)\} - \frac{\partial}{\partial x_i}\{[P_{ij} n_j + \rho u_i (u_n - v_n)]\delta(f)\} + \frac{\partial}{\partial t}\{[\rho_0 u_n + \rho(u_n - v_n)]\delta(f)\} \qquad (6)$$

where u_i and v_i are surface velocity components in x_i direction, u_n and v_n are fluid velocity components normal to the surface, $\delta(f)$ is Dirac delta function and, $H(f)$ is the Heaviside function [13].

3 Methodology

The baseline case is established by comparing OASPL results with the experimental study of the standard M219 cavity case. Henshaw [11] studied M219 cavity configurations in wind tunnel experiments—cavity setup in a rigging plate. The centreline of the rig plate is offset by 1 inch from that of a cavity. These configurations had 20×4 (length to width) and two depths of 4 in. (deep configuration) and two in. (shallow configuration). Ten static pressure measurement transducers were used on the bay ceilings with a 2-inch gap. For deep bay, these transducers lie on the rig's center line; for shallow bay, these transducers lie on the

cavity's centreline. Fig. 1 shows that K20 to k29 transducers are represented by monitoring points ku1 to ku10 in the CFD analysis of this study. These locations collect static pressure histories that are later processed for RMS values and OASPL levels.

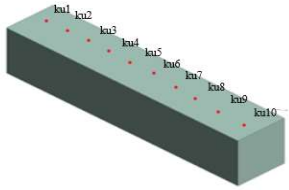

Fig. 1 Monitoring points location on cavity ceiling

This study uses CFD analysis to obtain the flow field for both configurations. The computational domain is simplified by only maintaining the cavity and rig plate's top surface. This is done to avoid any flow field disruptions for flow approaching the cavity itself due to the presence of rig setup. Fig. 2. shows y-x mesh refining towards the cavity. k-ω SST is a turbulence model with boundary conditions of velocity inlet, pressure outlet, and zero shear, adiabatic walls. The cavity and rig plate are no-slip walls. A hexa mesh is developed on the domain using a multizone meshing technique. The domain is decomposed into five blocks. A mesh density block that spans the area around the cavity is also developed. This region contains a mesh size similar to cells within the cavity. Mesh refines towards the cavity and coarsens out in the rest of the domain. The mesh cell count is around 2.88 million.

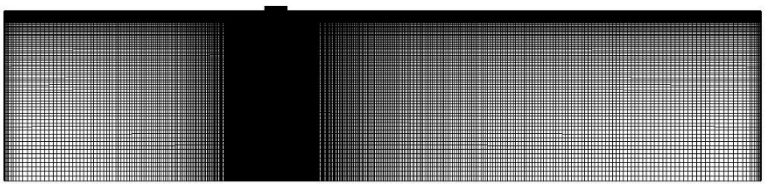

Fig. 2 y-x view of domain mesh

Table 1. gives flow variables and solver parameters used in these simulations. Computations start with an initial steady analysis to develop the flow within the domain. Then, transient simulation is set up with a small time step of 3e-05 for 0.15 seconds, which makes static pressure fluctuations complete a few periodic or pseudo-periodic cycles. An initial transient turbulent flow field was developed for almost 0.03 seconds (1000 time steps) for noise calculation in the far-field. FW-H model was turned on with cavity as a noise source and three receivers in uniform flow-field.

Table 1. Flow and solver parameters

Mach number	0.6
Velocity, U∞ (m/s)	202.86
Static pressure (Pa)	78699.7
Static temperature (K)	284.5
Solver	Pressure based
Turbulence Model	k-ω SST
Pressure-velocity coupling	Coupled

This study used the FW-H mid-to-far field acoustic model to obtain noise radiated by both cavities at three different receiver locations at different points of 1-meter vector rotation

around the cavity at the center of the cavity's top surface, as shown in Fig.3. These receivers are placed at this distance to experience a uniform flow field as FW-H-type integral-based methods require. These three receivers lie in the far-field region of the rear cavity since acoustic waves travel upstream of the flow [11].

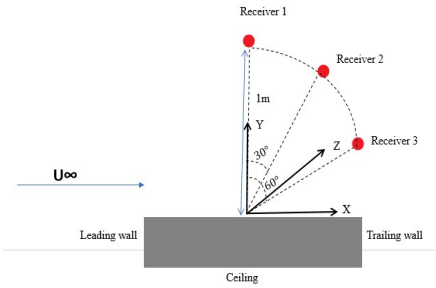

Fig. 3 Receiver location in far-field

4 Results and Discussion

This section analyzes results from intensive calculations using the coefficient of pressure Cp plots and contours. Further assessment is made by processing static pressure histories regarding SPL loads, as is customary cavity flow studies [14]. An effort is made to categorize these both bays into modes of operation. Aerodynamic drag and far-field noise are also estimated.

4.1 OASPL comparison

Pressure time histories collected from CFD simulations are post-processed to give OASPL levels, as is a trend in cavity flow studies to represent rms of static pressure as SPL loads. Prms are obtained from these static pressure histories from (6).

$$\mathrm{Prms} = \sqrt{\sum_{n=1}^{N} \frac{(\bar{p}-p)^2}{N}} \qquad (7)$$

Here, $\bar{p}$ is static pressure, p is instantaneous static pressure, and N is the number of time steps. Prms is measured in pascals, but studies in literature report rms values in terms of Overall Sound Pressure Levels (OASPL) [12] [13] [14] from (7).

$$\mathrm{OASPL} = 20\mathrm{LOG}_{10}\left[\frac{\mathrm{Prms}}{\mathrm{Pref}}\right] \qquad (8)$$

where, $Pref = 2 \times 10^{-5}$ is the international standard for minimum audible sound.

Figures 4 and 5 compare experimental data for both deep and shallow bays, respectively.

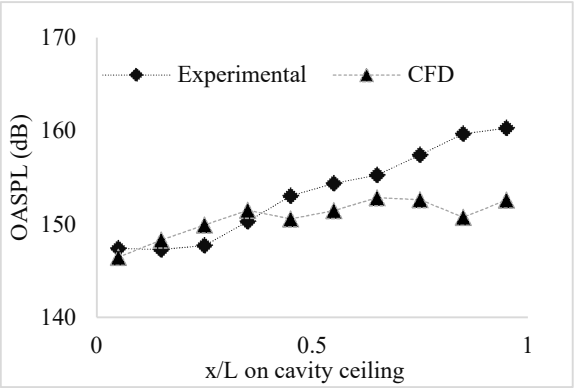

Fig. 4 OASPL along the deep bay ceiling

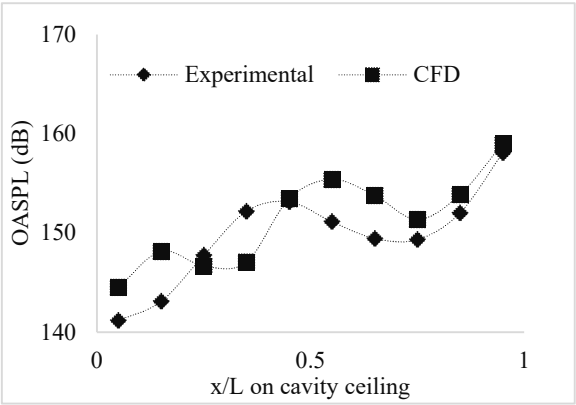

Fig. 5 OASPL along the shallow bay ceiling

A similar error is reported in the literature using RANS and Scale Resolving techniques [14]. This is because RANS averages out fluctuations, reducing its sensitivity to capture flow physics that depends on fluctuations. However, it has shown better results in the first half of the deep bay and at most monitoring points in a shallow bay. It is known from wind tunnel studies that shallow bays have lesser fluctuating pressures than deep bays.

A look into the longitudinal static pressure field as obtained in terms of Cp contours shown in Figure 6 clearly indicates areas of the cavity that suffer intense pressures and, subsequently, acoustic loads. A shallow bay also indicates a smaller recirculation (small blue region of negative pressure) region developed after trailing the wall of the cavity onto the plate.

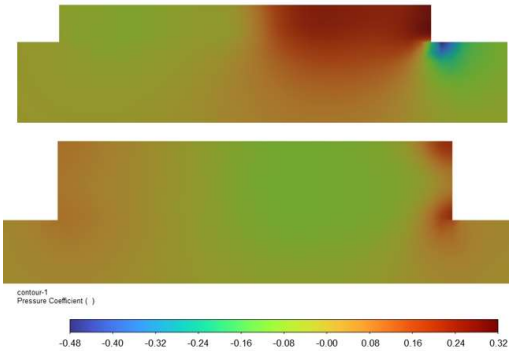

Fig. 6 Static pressure field in shallow (above) and deep (below) cavity on y-x plane

As the shear layer impinges on the deep bay, corners near the trailing wall suffer from intense pressure and acoustic loading of around 160 dB. The leading wall region, however, is much calm with 146 dB magnitude. In the shallow bay, after x/L 0.5, intense pressure loading can be seen in Fig. 6. This is the region where the shear layer separates after attachment, as visible in Figure 7.

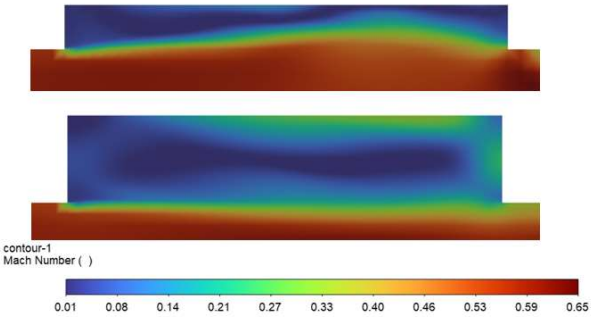

Fig. 7 Mach contours on shallow (above) and deep (below) bay

4.2 Cp distribution

Fig. 8 shows Cp profile obtained on monitoring points locations. A non-dimensional parameter of x/L is used for generic understanding as in experimental data.

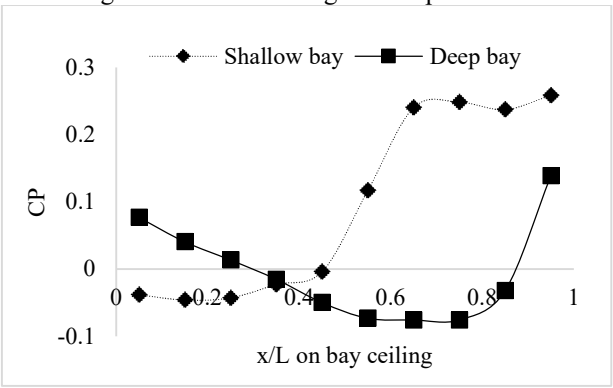

Fig. 8 Cp profile on ceiling of deep and shallow cavities

It can be seen that the deep bay shows much more pressure distribution than the shallow bay. This can be very well explained with velocity vectors of both bays, as shown in Fig. 9.

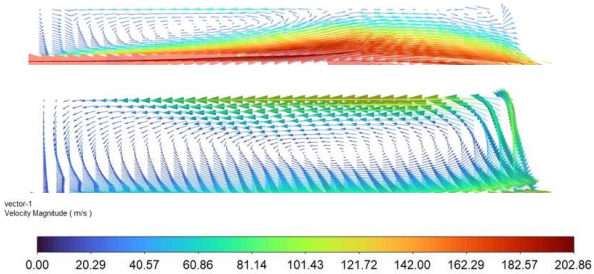

Fig. 9 Velocity vectors in shallow (above) and deep bay (below)

In the shallow bay, two recirculation regions develop. One relatively larger vortex is near the leading wall of the cavity, and one smaller eddy is trapped near the trailing wall of the cavity. These vortices enforce uneven pressure profiles. The recirculation region near the leading wall can oscillate residing store by creating downwash. Subsequent ejection of stores from such bays can be dangerous without any flow actuation as weapons can release with pitch-up motion. Deep bay, on the other hand, has one sizeable recirculating region spanning the whole cavity. Such a flow field is less likely to induce any pitching moment, given that stores are placed at x/L lengths of 0.3 to 0.8.

4.3 Drag due to bays

The mean drag coefficient obtained for the deep bay is 0.0030, and for the shallow bay is 0.016. As L/D increases, open cavities start to show bluff body type drag. A trapped eddy near the trailing wall and a larger vortex near the leading wall have degraded the aerodynamic efficiency of a shallow bay.

4.4 Far-field noise emission by bays

There is no currently valid data, but if a certain mesh and computational framework can solve near-field fluctuations with the required accuracy, it should be able to resolve OASPL levels in the far field with the help of the integral technique. As discussed earlier, cavities emit noise as monopole sources, and these three receivers near each other should receive comparable noise patterns. Fig. 10 and 11 give SPL distribution over frequencies at these receiver locations for deep and shallow cavities, respectively. It shows both cavities as a monopole acoustic source with the same noise radiation in a circular pattern. Table 2 agrees with the analogy for OASPL levels in the far field.

Table 2. OASPL at the receiver location

	Receiver 1 (dB)	**Receiver 2 (dB)**	**Receiver 3 (dB)**
Deep	126.67	126.825	122.712
Shallow	126.511	126.368	121.733

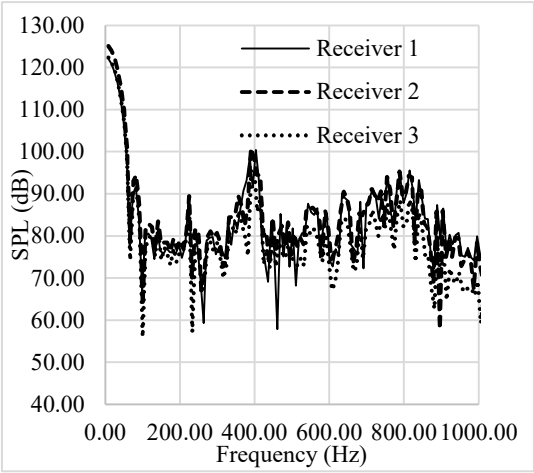

Fig. 10 SPL envelop at receiver location (shallow bay)

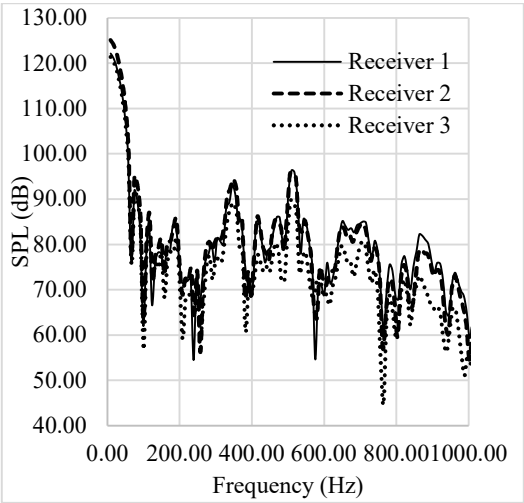

Fig. 11 SPL envelop at receiver location (deep bay)

5 Conclusion

After a comparative study of two 3d cavities with L/D of 4 and L/D of 10 at Mach 0.6, several conclusions can be drawn. First, the bay with an L/D of four at Mach 0.6 generally operates in shear layer mode, whereas the bay with an L/D of 10 operates in wake mode. Shallower bays show a drastic increase in drag and a tendency to induce pitch-up motion in housing stores. The difference in magnitude of OSPL loads on the ceiling of both cavities is negligible. Finally, both cavities show circular noise distribution patterns and act like monopole sound sources with no significant difference in SPL levels.

References

[1] L.Shaw, "Active control for cavity acoustics," in *AIAA/CEAS Aeroacoustic Conference*, 1998.

[2] S. Jr.L.Shaw, "Active Control of Shallow cavity acoustic resonance," in *Fluid Dynamics Conference*, 1996.

[3] J. Rossiter, "Wind Tunnel Experiments of flow over rectangular cavities on subsonic and transonic regimes," Ministry of Aviation, London, 1965.

[4] R. A. &. F. Mendonca, "DES Validations of Cavity Acoustics over the Subsonic to Supersonic Range," in *Aeroacoustic Conference*, 2004.

[5] G. Nampelly, "Surface Roughness Efects on Cavity Flows," *Flow, Turbulence and Combustion,* no. 109, pp. 1215-1239, 2022.

[6] M. J. d. C. Henshaw, "M219 Cavity Case," British Aerospace Ltd., Military Aircrafts and Aerostructures, 1991.

[7] M. G. a. A. Roshko, "The Effect of Flow Oscillations on Cavity Drag," *Journal of Fluid Mechanics,* Vols. 501-530, pp. 501-530, 1987.

[8] Y. L. Q. C. L. I. U. L. T. K. Sun, "Efects of sidewalls and leading-edge blowing on fows over long rectangular cavities," *AIAA Journal,* vol. 57, no. 1, pp. 106-119, 2019.

[9] A. B. B. J. &. R. L. S. Jr, "Cavity Door Effects on Aerodynamic Loads of Stores Separating from Cavities," *Journal of Aircraft,* vol. 26, no. 7, 1989.

[10] D. B. A. J. S. B. N. &. N. J. T. K Knowles, "Controlling unsteady cavity flow using internal structures," in *International Conference on Applied Aerodynamics*, Lyon, France, 2017.

[11] C. B. &. D. J. X. Gloerfelt, "Direct computation of the noise radiated by a subsonic cavity flow and application of integral methods," *Journal of sound and vibrations,* vol. 266, no. 1, pp. 119-146, 2003.

[12] M. Lighthill, "On Sound Generated Aerodynamically," in *Royal Society*, London, 1952.

[13] L. Hawkings, "Sound Generation by Turbulence and Surfaces in Arbitrary," in *Royal Society*, London, 1969.

[14] G. N. B. a. N. J. T. G. J. M. Loupy, "Cavity Flow over a TransonicWeapons Bay During Door Operation," *Journal of Aircrafts,* 2017.